Flexible and curtailable resource activation in a distribution network using nodal sensitivities

Md Umar Hashmi, Arpan Koirala, Hakan Ergun, Dirk Van Hertem
KU Leuven & EnergyVille, Genk, Belgium
(mdumar.hashmi, arpan.koirala, hakan.ergun, dirk.vanhertem)@kuleuven.be

Abstract—Traditionally, the distribution system operator (DSO) relied on a fit-and-forget network design. However, there will be a greater need to integrate flexible and curtailable resources to cope with growing distributed generation (DG) installations and new consumer loads such as electric vehicles. Distribution network (DN) vulnerabilities, voltage and thermal limit violations, often require resource activation in the vicinity. Consumers located close to the end of the feeder in a radial DN witness more over-voltages (due to DG injection) and under-voltages (due to additional load). The per-unit change in active or reactive power of a consumer at the end of the feeder causes a greater marginal impact, referred to as nodal sensitivity. This will cause a higher activation of flexible resources close to the vulnerable nodes. A flat flexible activation priority will not be fair for such flexible owners. We propose a new mechanism to activate flexibility based on voltage sensitivity which considers nodal sensitivities. The proposed activation design is motivated by inverter voltage control norms and has similarities with optimal power flow duals often utilized as locational marginal prices. These dual variables are active only when some network constraints are violated and do not provide correction prior to such a violation. The proposed flexibility activation design, due to its drooping characteristics actively contributes to avoiding such network issues from happening. The resource activation optimization formulation proposed is non-convex. Second-order cone relaxations are used to convexify the proposed resource activation optimization problem. We use numerical evaluations to show the proposed formulations can be used for activation of load flexibilities and can be used for valuing and planning flexible and curtailable resources.

Index Terms—Flexibility, load curtailment, optimal power flow (OPF), convex optimization, locational marginal price (LMP)

I. INTRODUCTION

The growing variability in power system due to weather dependent renewable generation will require more resources which can be used to increase or decrease consumption. These resources could be either flexibility or curtailable resources. Interruptible installations are being promoted by different DSOs and retailers in Europe. In Germany, Mitnetz Storm under section 14a of German energy act (EnWG) provides discounts on grid usage charge and volumetric component for consumer interruptible installations such as heat pumps, electric heating etc [1]. In Belgium, Luminus in Flanders region provides exclusive night charges for consumers which are more than 28% cheaper compared to single rate meter charges [2]. With growing distributed generation, the need for flexible resources is critical for reliable operation of DN.

Developing a business case for the growth of such flexible resources by appropriately designing electricity markets will promote the growth of flexible resources while ensuring their profitability [3]. In this work we propose hierarchical flexible and curtailable resource activation mechanism. Resources participating in such a market have a lower temporal priority such as water heaters, HVAC systems, thermostatic loads, pool pumps, batteries etc [4].

Authors in [5] indicate that due to lack of location specific electricity market design, system operators cannot avail load flexibility for balancing or congestion services. They identify three ways of utilizing DN flexible resources: (a) utilize existing wholesale market for contracting flexibility, (b) create an independent flexibility market and (c) use a market approach similar to reserves. Our work is close to the second category where only more responsive loads/energy storage and low temporal priority loads participate in the flexibility market, thus facilitating real-time location-aware DN operation [6].

Voltage sensitivity towards active and reactive power is an extensively researched topic. Voltage sensitivities are often calculated for estimating the marginal impact of adding or removing active or reactive power at a node. In this way, load flexibility [7], DG inverter operation [8]–[11], battery management [12]–[14], capacitor placement [15], on-line load sensitivity [16], implementations can be performed using local control without installing central communication for feedback. In this work we use voltage sensitivity towards active and reactive power in order to design priorities for flexible resource activation in the DN. These activation priorities are analogous to LMPs. In this work, we consider only the variable component of such LMPs, DSO may also need to settle the capacity cost even if the flexibility is not utilized. The capacity cost itself is not considered in this work. Further, the market operator may need to create a framework to measure the performance of flexible resources when requested to activate, similar to an ancillary services market operated under PJM in the US [17]. In this work we assume full performance by resources when activated depending on their reported limits.

Similar to [18], this paper assumes that instantaneous flexibility in the form of lower and upper envelopes are known to DSO, e.g., provided by an intermediary actor as a resource aggregator. Here we focus on flexible and subsequently curtailable resource activation using the proposed flexibility activation priority design which takes into account the nodal voltage sensitivity, local voltage measurement and connected line loadings. The proposed resource activation methodology can be used by DSOs to quantify the need and the value of different flexible resources in the DN. The flexibility activation priority maybe cleared in the energy market and the DSO can use this framework for valuing flexible resources for market-clearing. Note that with

local measurement of line currents and nodal voltages used in the proposed activation signal design, it can be used in a distributed manner without the need for DSOs to communicate activation signals, which will be the future direction of this work.

The paper is organized as follows. Section II presents the load sensitivity matrix calculations for active and reactive power perturbations. Section III presents the model used for calculating the flexibility activation signal. Section IV formulates the optimization problem for resource activation using second-order cone relaxation. Section V presents the numerical results an section VI concludes the paper.

II. SENSITIVITY OF NODES

The voltage sensitivity matrix can be calculated using (a) Jacobian-matrix inverse based on linearized power flow equations used in the Newton-Raphson power flow, (b) perturb and observe method, (c) admittance compound matrix [19], (d) fitting-function based sensitivity approach [10].

The Newton-Raphson power flow equations are denoted as $\begin{bmatrix} \Delta P \\ \Delta Q \end{bmatrix} = J \begin{bmatrix} \Delta \theta \\ \Delta V \end{bmatrix}$ where the Jacobian-matrix inverse is

$$ J^{-1} = \begin{bmatrix} \partial \theta / \partial P & \partial \theta / \partial Q \\ \partial V / \partial P & \partial V / \partial Q \end{bmatrix}. \quad (1) $$

We use the *perturb-and-observe* method which approximates sensitivity components for the nodal voltage as shown in (1) using small perturbations in active and reactive power and observing voltage magnitude changes.

A. Notation

A power network is composed of several components such as nodes, branches, generators and loads. A network is characterized by $< N, E >$, where N denotes nodes and E denotes branches connecting pair of nodes. Each node $i \in N$ and time t has two variables, i.e., voltage magnitude ($V_{i,t}$) and phase angle ($\theta_{i,t}$) which are governed by power injection and load magnitude. The branch admittance $(i, j) \in E$ governs the flow and losses. Nodes with loads connected is denoted as $N_L \subset N$. These nodes have active and reactive power loads denoted as $P_{i,t}^d$ and $Q_{i,t}^d$. Nodes with generators connected is denoted as $N_G \subset N$, have active and reactive power generation denoted as $P_{i,t}^g$ and $Q_{i,t}^g$. $|.|$ denotes the absolute value.

B. Voltage sensitivity

The voltage sensitivity matrix with active and reactive power load fluctuation is defined as

$$ \Psi_{hk} = \left| \frac{V_k - V_{k0}}{P_h - P_{h0}} \right|, \quad \beta_{hk} = \left| \frac{V_k - V_{k0}}{Q_h - Q_{h0}} \right|, \ h, k \in N. \quad (2) $$

where the active load at node h is modified from P_{h0} (Q_{h0}) to P_h (Q_h), due which the new power flow results in change in voltage at each node $k \in N$. V_{k0} denotes the voltage at node k corresponding to load P_{h0} (Q_{h0}).

Averaging: Note that value of Ψ_{hk} and β_{hk} depends on reference load P_{h0} and Q_{h0}. [7] indicate that higher network loading implies greater voltage sensitivity. In order to eliminate the loading effects Ψ_{hk} and β_{hk} are calculated at different loading conditions and averaged over a large number of simulations.

III. ACTIVATION OF FLEXIBILITY IN DN

Activation of flexible resources is crucial for healthy operation of DNs with DGs and new loads which will be more prone to thermal violations, under-voltage and over-voltage phenomenons. Firstly, DN's locational aspect needs to be considered so as flexibility owners are fairly valued for their responsive services. Secondly, the flexible resources need to be activated only when there are grid issues or when the network state is close to voltage or thermal violations at one or more nodes. Considering these aspects we propose a flexibility activation priority design combining voltage sensitivities shown in (2) with instantaneous network states. These sensitivity values are analogous to merit-order for flexibility activation. In a radial distribution network, the sensitivity at the end of the feeder will be significantly higher than the voltage at the beginning of the feeder. Due to this reason, the probability of voltage incidents is higher close to the end of the feeder.

The proposed priority value of flexibility is governed by network state. If there are voltage and/or thermal violations in the network, the value of flexibility is non-zero in magnitude while it is zero when there are no violations. The structure of flexibility value is shown in Figure 1. The flexibility activation signal follows a drooping behavior similar to P(V) (volt-watt) and Q(V) (volt-var) inverter control used in operation of active DNs [20], [21]. The active and reactive power flexibility activated by the DSO are given as

$$ \Delta P_{i,t}^{\text{flex}} \in [P_{\min,i,t}^{\text{flex}}, P_{\max,i,t}^{\text{flex}}], \ \Delta Q_{i,t}^{\text{flex}} \in [Q_{\min,i,t}^{\text{flex}}, Q_{\max,i,t}^{\text{flex}}]. \quad (3) $$

From Fig. 1 we observe that ramping up or ramping down of flexible resources at any particular time will be governed by the nodal voltage and the thermal loading of branches connected to the node. It is essential to separate active and reactive flexibilities into capacitive and inductive components for reactive power and absorption and injection for active power for ensuring the correct direction of compensation is provided. These variables are

$$ \Delta P_{i,t}^{\text{flex}+} \in [0, P_{\max,i,t}^{\text{flex}}], \quad \text{(active power injection)}, \quad (4a) $$
$$ \Delta P_{i,t}^{\text{flex}-} \in [P_{\min,i,t}^{\text{flex}}, 0], \quad \text{(active power consumption)}, \quad (4b) $$
$$ \Delta Q_{i,t}^{\text{flex}+} \in [0, Q_{\max,i,t}^{\text{flex}}], \quad \text{(reactive power injection)}, \quad (4c) $$
$$ \Delta Q_{i,t}^{\text{flex}-} \in [Q_{\min,i,t}^{\text{flex}}, 0], \quad \text{(reactive power consumption)}. \quad (4d) $$

Thus, $\Delta P_{i,t}^{\text{flex}} = \Delta P_{i,t}^{\text{flex}+} + \Delta P_{i,t}^{\text{flex}-}$ and $\Delta Q_{i,t}^{\text{flex}} = \Delta Q_{i,t}^{\text{flex}+} + \Delta Q_{i,t}^{\text{flex}-}$. Clearly, the directionality of the network will reverse P and Q compensation strategies if the power flow direction reverses. For example, for a network with low load and large DG generation this can lead to a reversed power flow.

The proposed mechanism to prioritize operational flexibility considers instantaneous network state in terms of nodal voltages and branch thermal loadings. Note that thermal loadings are associated with branches and the proposed flexibility activation signals are *nodal*. For an overloaded line, the thermal component of the flexibility activation signal is included in nodal activation of both nodes connected to the congested branch. The details of how the thermal loading of branches are projected into nodes is described in Section III-A. The upper bound of the voltage component of the active power flexibility activation signal is

shown in Fig. 1 is denoted as $\text{VC}_{i,P}^{\max}$ and the thermal component is denoted as $\text{TC}_{i,j,P}^{\max}$.

$$\text{VC}_{i,P}^{\max} = f_P(\Psi_P), \ \text{TC}_{i,j,P}^{\max} = g_P(\beta_P). \tag{5}$$

Similarly, the reactive component of the flexibility value due to voltage and thermal limit violation is denoted as

$$\text{VC}_{i,Q}^{\max} = f_Q(\Psi_Q), \ \text{TC}_{i,j,Q}^{\max} = g_Q(\beta_Q). \tag{6}$$

Fig. 1 denotes a generic flexibility prioritization mechanism with following parameters defined as:

- ΔT_{perm}: denotes permissible thermal loading below which DSO does not activate flexibility,
- ΔV_{perm}: denotes the dead-band across 1 pu desired voltage at a node for which DSO does not activates flexibility.

Although for this work, ΔV_{perm} is considered symmetrical around 1 per unit voltage, it can be asymmetrical. The flexibility activation value for active power ramp up and ramp down is denoted as

$$\lambda_{i,t}^{\text{flex}_P+} = 1\left(V_{i,t}^{\text{inst}} \leq V_{\min}\right)\text{VC}_{i,P}^{\max} + 1\left(T_{i,j,t}^{\text{inst}} \geq 100\right)\text{TC}_{i,j,P}^{\max} +$$

$$1\left(V_{i,t}^{\text{inst}} \in (V_{\min}, 1-\Delta V_{\text{perm}})\right)\frac{\text{VC}_{i,P}^{\max}\left(V_{i,t}^{\text{inst}} - (1-\Delta V_{\text{perm}})\right)}{\left(V_{\min} - (1-\Delta V_{\text{perm}})\right)} +$$

$$1\left(T_{i,j,t}^{\text{inst}} \in (\Delta T_{\text{perm}}, 100)\right)\frac{\text{TC}_{i,P}^{\max}\left(T_{i,t}^{\text{inst}} - \Delta T_{\text{perm}}\right)}{\left(100 - \Delta T_{\text{perm}}\right)} \tag{7a}$$

$$\lambda_{i,t}^{\text{flex}_P-} = 1\left(V_{i,t}^{\text{inst}} \geq V_{\max}\right)(-\text{VC}_{i,P}^{\max}) + 1\left(T_{i,j,t}^{\text{inst}} \geq 100\right)(-\text{TC}_{i,j,P}^{\max})$$

$$+ 1\left(V_{i,t}^{\text{inst}} \in (1+\Delta V_{\text{perm}}, V_{\max})\right)\frac{(-\text{VC}_{i,P}^{\max})\left(V_{i,t}^{\text{inst}} - (1+\Delta V_{\text{perm}})\right)}{\left(V_{\max} - (1+\Delta V_{\text{perm}})\right)}$$

$$+ 1\left(T_{i,j,t}^{\text{inst}} \in (\Delta T_{\text{perm}}, 100)\right)\frac{(-\text{TC}_{i,P}^{\max})\left(T_{i,t}^{\text{inst}} - \Delta T_{\text{perm}}\right)}{\left(100 - \Delta T_{\text{perm}}\right)} \tag{7b}$$

The expression 1(condition) denotes an indicator function which returns 1 if the condition is true and 0 otherwise. The flexibility activation value for reactive power, $\lambda_{i,t}^{\text{flex}_Q+}$ and $\lambda_{i,t}^{\text{flex}_Q-}$, can be derived in a similar manner as shown in (7). Note that $\lambda_{i,t}^{\text{flex}_P+}$ is associated with $\Delta P_{i,t}^{\text{flex}+}$ and so on (see (12)). For rotational simplicity we use $\lambda_{i,t}^{\text{flex}}$ denoting the set of flexibility activation signals for time t and node i as $\{\lambda_{i,t}^{\text{flex}_P+}, \lambda_{i,t}^{\text{flex}_P-}, \lambda_{i,t}^{\text{flex}_Q+}, \lambda_{i,t}^{\text{flex}_Q-}\}$.

A. Nodal projection of thermal branch loading

The power flow direction from the substation transformer to prosumers in a radial DN as positive. Due to DG integration in DN, reverse flow occurs when DGs generate more power than power consumed by connected loads. The reverse power flow can be localized to a portion of the DN. It is crucial to correctly identify the direction of the power flow in order to ensure flexible resource activation does not aggravate the DN issues. For example, if a line is overloaded with reverse power flow, then generation needs to be curtailed rather than load or load needs to be increased. In algorithm III-A we identify the flow direction based on nodal voltage magnitudes. Then based on

these flow values we propose a load projection from branches into nodes. Some nodes may be connected to more than one branch, for which the nodal projection is denoted as

$$\text{Nodal Loading} = \frac{\sum_{\text{lines connected}} (\text{line loading})\,(\text{line rating})}{\sum_{\text{lines connected}} (\text{line rating})}. \tag{8}$$

b_{yz} denotes a branch connecting node y to z. The flow direction is identified using nodal voltage magnitudes as

$$\zeta_{b_{yz}} = 1(V_y \geq V_z) - 1(V_z > V_y), \tag{9}$$

where V_y denotes voltage magnitude at node y.

Algorithm 1 `Nodal Projection of Loading`

Inputs: Loading matrix, flow convention, network voltage matrix
1: Update loading matrix considering flow directions using flow convention captured using (9),
2: Project line loadings into nodes using (8),
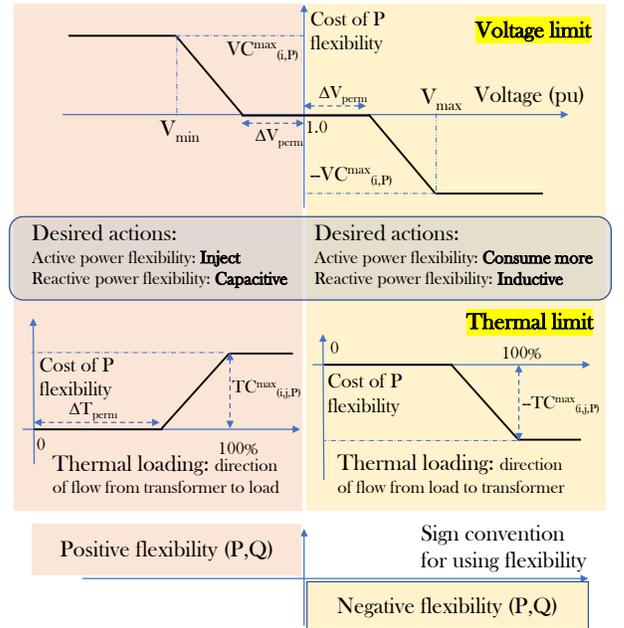3: Calculate & return thermal component of flex activation signals.

Fig. 1. Value of flexibility at node i derived based on voltage deviation and thermal loading. ΔT_{perm}: denotes permissible thermal loading below which DSO does not activate flexibility, ΔV_{perm}: denotes the dead band across desired voltage for which DSO does not activates flexibility, $V_{\min}, V_{\max}$: the minimum and maximum voltage level.

B. Flexibility constraints: re-definitions

The ramp up and ramp down flexibility constraints are defined in (4). Note that ramp up and ramp down variables are separated to represent $\Delta P_{i,t}^{\text{flex}}$ and $\Delta Q_{i,t}^{\text{flex}}$. This implies for active flexibility either $\Delta P_{i,t}^{\text{flex}+}$ or $\Delta P_{i,t}^{\text{flex}-}$ could be non-zero at any time t. Similarly for reactive power either $\Delta Q_{i,t}^{\text{flex}+}$ or $\Delta Q_{i,t}^{\text{flex}-}$ could be non-zero at any time t. Further, for cases where $\lambda_{i,t}^{\text{flex}_P+}, \lambda_{i,t}^{\text{flex}_P-}$ are both zero implying voltage and line loadings are within permissible bounds, both $\Delta P_{i,t}^{\text{flex}+}$ and $\Delta P_{i,t}^{\text{flex}-}$ should be zero. Similarly, for cases where $\lambda_{i,t}^{\text{flex}_Q+}, \lambda_{i,t}^{\text{flex}_Q-}$ are both zero implying voltage within permissible bounds, $\Delta Q_{i,t}^{\text{flex}+}$ and $\Delta Q_{i,t}^{\text{flex}-}$ should be zero. In absence of the above conditions

being considered, the power balance constraint in optimal power flow implementations will not accurately represent the system. This problem can be solved by introducing an integer variable in the DSO optimization problem or by redefining the flexibility constraint in (4) as

$$\Delta P_{i,t}^{\text{flex}+} \in [0, z_1 P_{\max,i,t}^{\text{flex}}] = [0, P_{\max,i,t}^{\text{flex}N}], \tag{10a}$$

$$\Delta P_{i,t}^{\text{flex}-} \in [z_2 P_{\min,i,t}^{\text{flex}}, 0] = [P_{\min,i,t}^{\text{flex}N}, 0], \tag{10b}$$

$$\Delta Q_{i,t}^{\text{flex}+} \in [0, z_3 Q_{\max,i,t}^{\text{flex}}] = [0, Q_{\max,i,t}^{\text{flex}N}], \tag{10c}$$

$$\Delta Q_{i,t}^{\text{flex}-} \in [z_4 Q_{\min,i,t}^{\text{flex}}, 0] = [Q_{\min,i,t}^{\text{flex}N}, 0], \tag{10d}$$

where z_1, z_2, z_3, z_4 denotes binary variables. These binary variables are calculated as

$$z_1 = 1(\Delta\lambda_{i,t}^{\text{flex}P+} \neq 0), z_2 = 1(\Delta\lambda_{i,t}^{\text{flex}P-} \neq 0),$$
$$z_3 = 1(\Delta\lambda_{i,t}^{\text{flex}Q+} \neq 0), z_4 = 1(\Delta\lambda_{i,t}^{\text{flex}Q-} \neq 0). \tag{11}$$

Since the activation signals are calculated prior to solving resource dispatch optimization problem, the flexibility box constraints are defined according to (10) which avoids the inclusion of binary variables in the resource dispatch problem, such that binary variables z_1, z_2, z_3, z_4 become parameters.

IV. RESOURCE ACTIVATION

The DSO makes the decision to activate a flexible resource reported at each individual node within a lower and upper flexibility envelope. The DSO aims to reduce active power losses, reduce the activation value of flexibility and curtailment of generation and load while ensuring voltage limits, power balance, thermal limits, Ohm's law, phase angle, flexibility ramping, load and generation curtailment limit constraints.

Optimization formulation: The decision variables for the optimization are $\Gamma = \{P_{j,t}^g, \Delta P_{i,t}^{\text{flex}}, \Delta Q_{i,t}^{\text{flex}}, \Delta P_{i,t}^{\text{curt}}, \Delta P_{i,t}^{\text{G}}\}$ which denote active power flexible resource activated, reactive power flexible resource activated, active power generation curtailment and load shedding, respectively.

The objective function for time t is given as

$$\sigma(w_i, P_{j,t}^g, \rho, \lambda_{i,t}^{\text{flex}}, \lambda_{i,t}^{\text{curt}P}, \lambda_{i,t}^{\text{curt}G}) = \sum_{j \in N_G} C_G(P_{j,t}^g) + w_1\rho(t)$$
$$+ w_2\lambda_{i,t}^{\text{flex}P+} \sum_{i \in N} \Delta P_{i,t}^{\text{flex}+} + w_3\lambda_{i,t}^{\text{flex}P-} \sum_{i \in N} \Delta P_{i,t}^{\text{flex}-}$$
$$+ w_4\lambda_{i,t}^{\text{flex}Q+} \sum_{i \in N} \Delta Q_{i,t}^{\text{flex}+} + w_5\lambda_{i,t}^{\text{flex}Q-} \sum_{i \in N} \Delta Q_{i,t}^{\text{flex}-} +$$
$$w_6\lambda_{i,t}^{\text{curt}G} \sum_{i \in N} \Delta P_{i,t}^{\text{G}} + w_7\lambda_{i,t}^{\text{curt}P} \sum_{i \in N} \Delta P_{i,t}^{\text{curt}}, \tag{12}$$

where $C_G(.)$ denotes the generator cost function, ρ denotes line losses, $w_i \; \forall \; i$ denotes weights corresponding to different components of the objective function. We can select the objective function parameter values as follows:

$$0 \leq \max(\lambda_{i,t}^{\text{flex}P+}, |\lambda_{i,t}^{\text{flex}P-}|) < \lambda_{i,t}^{\text{curt}G}, \lambda_{i,t}^{\text{curt}P}. \tag{13}$$

(13) ensures that no load shedding is performed before availing other options. Authors in [22] use active and reactive power sensitivities for approximating the R/X ratio which governs the importance of reactive power compared to reactive power. In

this work we assume this is captured by values of (5) and (6). The full nonlinear optimization formulation (AC flex OPF) is denoted as P_{org} and given as

$$\min_{\Gamma} \sum_t \sigma(w_i, P_{j,t}^g, \rho, \lambda_{i,t}^{\text{flex}}, \lambda_{i,t}^{\text{curt}P}, \lambda_{i,t}^{\text{curt}G}) \tag{14a}$$

subject to, Eq. 10 and

$$V_{\min}^i \leq |V_{i,t}| \leq V_{\max}^i, \; \forall i \in N, t \in \{1, .., T\}, \tag{14b}$$

$$(P_{i,t}^g - \Delta P_{i,t}^G) - (P_{i,t}^d - \Delta P_{i,t}^{\text{curt}} - \Delta P_{i,t}^{\text{flex}}) +$$
$$j(Q_{i,t}^d - \Delta Q_{i,t}^{\text{flex}}) = \sum s_{ij}^t, \quad \forall \; i, j \in N, \tag{14c}$$

$$|S_{ij}^t| < s_{ij}^{\max}, \quad \forall \; i, j \in N, \tag{14d}$$

$$P_{i,t}^g \in [P_{\min,i}^g, P_{\max,i}^g], \quad \forall \; i \in N_G, \tag{14e}$$

$$S_{ij}^t = \mathbf{Y}_{ij}^* V_{i,t} V_{i,t}^* - \mathbf{Y}_{ij}^* V_{i,t} V_{j,t}^*, \; \forall (i,j) \in E \cup E^R, \tag{14f}$$

$$\angle(V_{i,t} V_{j,t}^*) \in [\theta_{ij}^{\min}, \theta_{ij}^{\max}], \quad \forall \; i, j \in N, \tag{14g}$$

$$0 \leq \Delta P_{i,t}^G \leq P_{i,t}^g, \quad \forall i \in N_G, \tag{14h}$$

$$0 \leq \Delta P_{i,t}^{\text{curt}} \leq P_{i,t}^d, \quad \forall i \in N_L. \tag{14i}$$

(14b), (14d) and (14g) denote the voltage constraint for nodes, thermal constraint and phase angle constraints for branches, respectively. (14c) denotes the nodal balance of active and reactive power in the network. (14e) denotes the generator output power limits. (14f) denotes Ohm's law. Flexibility limits for active and reactive ramp up and ramp down are denoted in (10). (14h) and (14i) place limits on generation and load curtailment respectively.

A. Convexification of optimization

Optimization formulation P_{org} is non-convex due to (14b).

The voltage constraint in the power flow equations causes P_{org} to be nonlinear. Second order cone (SOC) relaxation according [23] is used to convexify the problem. This formulation is referred as SOC flex OPF:

$$|W_{ij}^t|^2 \leq W_{ii}^t W_{jj}^t, \; \text{where} \; V_{\min}^2 \leq W_{ii}^t \leq V_{\max}^2, \tag{15a}$$

$$S_{ij}^t = \mathbf{Y}_{ij}^* W_{ii}^t - \mathbf{Y}_{ij}^* W_{ij}^t, \; \forall (i,j) \in E \cup E^R \tag{15b}$$

The convex formulation of P_{org} is denoted as

$$(P_{\text{cvx}}) \quad \text{objective function} \quad \text{Eq. } 14a,$$
subject to , $(10), (15), (14c), (14d), (14g), (14e), (14h), (14i)$.

B. Ex-ante activation signals for real-time resource dispatch

Based on the network state, voltage values and thermal loadings, the flexibility activation signals are calculated. The cost of generation and load curtailment is set higher than the highest flexibility activation priority levels. The resource activation signals are used in solving P_{cvx}. Since the activation signal levels for flexibility and curtailment are set a priori to activation, therefore, referred to as ex-ante. Steps of *resource activation* are described in algorithm 2.

Algorithm 2 `Resource Activation`

Inputs: T, Network data, $t_{\text{samp}}, V_{\min}, V_{\max}, t = 0,, \Delta T_{\text{perm}}, \Delta V_{\text{perm}}$,
1: Calculate Ψ and β using (2),
2: Calculate $\text{VC}_{i,P}^{\max}, \text{VC}_{i,Q}^{\max}, \text{TC}_{i,P}^{\max}, \text{TC}_{i,Q}^{\max}$ using Eq. 5 and 6,
3: **while** $t < T$ **do**
4:   Input flexibility envelopes for active $[P_{\min,i,t}^{\text{flex}}, P_{\max,i,t}^{\text{flex}}]$ and reactive power $[Q_{\min,i,t}^{\text{flex}}, Q_{\max,i,t}^{\text{flex}}]$ for all nodes $i \in N$,
5:   Input load profiles for time t and perform load flow analysis,
6:   If no thermal or voltage violations at any nodes: go to Step 11,
7:   Calculate flexibility activation signals using voltage and line loading (in Step 4) using (7),
8:   Set generation and load curtailment cost using (13),
9:   Update flexibility ranges using (10),
10:   Solve P_{cvx} and activated flexibility is calculated as in (4),
11:   Increment $t = t + t_{\text{samp}}$,
12: **end while**
13: Return $\Delta P_{i,t}^{\text{flex}}, \Delta Q_{i,t}^{\text{flex}}, \Delta P_{i,t}^{\text{curt}}, \Delta P_{i,t}^{\text{G}}, \rho_t, \lambda_{i,t}^{\text{flex}}, \lambda_{i,t}^{\text{curt}P}, \lambda_{i,t}^{\text{curt}G} \forall i, t$.

V. NUMERICAL RESULTS

A simple test grid with 12 LV consumers (Fig 2 is used to show the numerical results. The main branch (0-2-5-8-11-14-17) are all assumed to be 150 sq mm Al cable 300 m per segment. The remaining branches connecting the main branch to LV consumers are assumed to be 35 sqmm Al cables of length 150 m each. The consumer features were selected to represent typical consumers in Belgium (Table I). The load profiles were selected from the real consumers of Belgium for a typical spring day and the PV profile were obtained from the irradiance data of EnergyVille roof-top in Genk, Belgium. The numerical
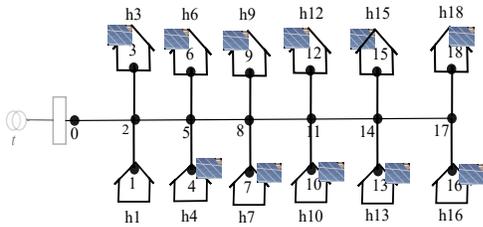
Fig. 2. Simplified network for numerical results

TABLE I
LV CONSUMER IN THE TEST FEEDER

prosumer	PV [kWp]	HP [kW]	SMEs	peak Load [kW]
h1	-	-	N	20
h3	10	-	Y	7
h4	20	-	N	4
h6	8	-	N	2
h7	20	-	Y	9
h9	12	-	N	12
h10	15	6	Y	14
h12	12	-	N	14
h13	10	-	N	14
h15	18	-	N	16
h16	18	-	N	20
h18	18	7.5	N	10

simulations are performed using PowerModels.jl in Julia / JuMP [24]. The aggregate load seen from the substation is shown in Fig. 3. The nodal P, Q nodal sensitivities for the network are shown in Fig. 4. Observe that prosumers connected at the end of the feeder have a greater P, Q sensitivity compared to nodes close to the transformer. Nodes with no prosumers connected are assumed to have no load flexibility, therefore, have sensitivities equal to zero.
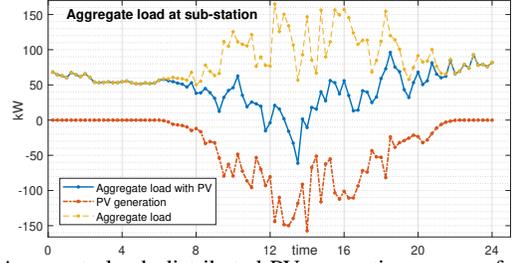
Fig. 3. Aggregate load, distributed PV generation as seen from substation transformer.
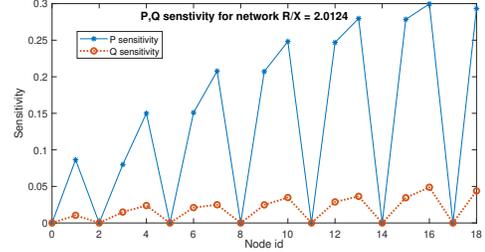
Fig. 4. Active and reactive power nodal sensitivity.

A. OPF duals vs flexibility activation signals

The dual variables of the optimal power flow problem are often used as locational marginal prices (LMP). These dual variables are active only when OPF constraints are reached as KKT conditions are active in such a case. The dual variables,
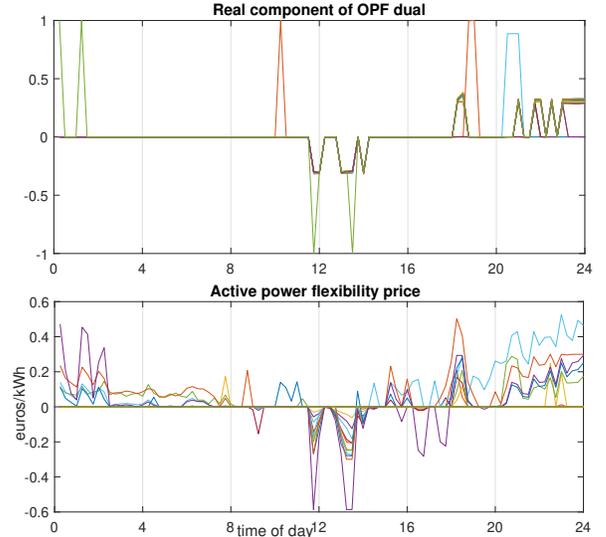
Fig. 5. OPF duals vs flexibility activation signals. The second plot shows the nodal flexibility value plotted over an entire day.

however, does not provide corrective feedback prior to OPF constraint violation. Our proposed flexibility activation signals holds some similarities as can be observed in Fig. 5. Proposed flexibility activation signals unlike the OPF duals actively try to correct network flow and voltage levels if they exceed permissible safe levels of operation.

B. Simulations with network voltage and thermal violation

Simulation results shows the efficacy of the proposed resource activation algorithm. Fig. 6 shows load and generation curtail-

ment in dependence of the load flexibility level for simulation horizon of 1 day. Asterisk indicate the level of load flexibility
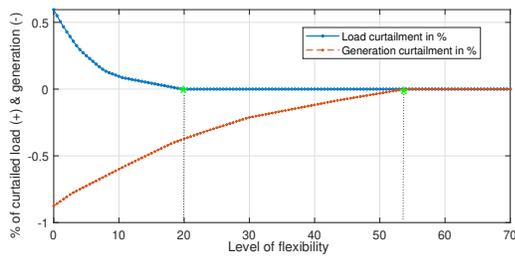

Fig. 6. Load and generation curtailment with varying level of flexibility

required for achieving zero load and generation curtailment. Similar studies with probabilistic permissible bounds on load and generation curtailment can be utilized for planning load flexibility needed for avoiding network issues.

C. Optimality gap: SOC relaxed vs nonlinear power flow

For loss costs = 0.67 Euro/kWh, generator and load curtailment cost of 0.47 and 0.87 Euro/kWh. The optimality gap between SOC and AC OPF is 0.0059%. The computation time for 19 bus network for SOC formulation is 3.016 sec and AC OPF is 3.391 sec. The small optimality gap is justified by 11.05% faster computation time required for SOC formulation. Computational advantage of solving SOC flex OPF would be be further analyzed in future works.

VI. Conclusion

We propose a flexible and curtailable resource activation and valuation mechanism that DSO's can use in flexibility planning, market clearing of flexible and curtailable resource. The proposed activation signal is motivated by P(V) and Q(V) inverter control method and therefore, bounded. The curtailed resources are valued greater than the highest flexibility activation signal. This ensures that no curtailment of load or generation prior to activating all available flexible resources takes place. The proposed flexibility activation signals are proportional to nodal sensitivities, therefore, flexible resources at more vulnerable nodes are valued more.

We observe that the proposed mechanism has similarities with the duals of OPF often used in LMP based approaches. Unlike, LMPs which are active only when some OPF constraint is reached, however, our proposed flexibility activation signals actively corrects nodal voltages and line loadings prior to any violation due to the drooping behavior (see Fig. 1). Numerical experiments show the efficacy of flexibility activation signal design and active and reactive power resource activation in a distribution network. Further, SOC relaxations for AC flex OPF can be justified due to low optimality gap and faster computation time, which will be more crucial for large DN feeders and towards real life, real time implementation.

Acknowledgement

References

[1] "Preisblatt 2 - Netzentgelte für Entnahmen ohne Leistungsmessung entgelte gültig ab 01.01.2021," https://tinyurl.com/rasefscy, accessed: 2021-02-25.

[2] "Tous les plans tarifaires luminus," https://tinyurl.com/4xhymdrd, accessed: 2021-02-25.

[3] J. Ma, V. Silva, R. Belhomme, D. S. Kirschen, and L. F. Ochoa, "Evaluating and planning flexibility in sustainable power systems," in *2013 IEEE power & energy society general meeting*. IEEE, 2013.

[4] Y. Chen, M. U. Hashmi, J. Mathias, A. Bušić, and S. Meyn, "Distributed control design for balancing the grid using flexible loads," in *Energy Markets and Responsive Grids*. Springer, 2018, pp. 383–411.

[5] A. Ramos, C. De Jonghe, V. Gómez, and R. Belmans, "Realizing the smart grid's potential: Defining local markets for flexibility," *Utilities Policy*, vol. 40, pp. 26–35, 2016.

[6] H. Hao and W. Chen, "Characterizing flexibility of an aggregation of deferrable loads," in *53rd IEEE Conference on Decision and Control*. IEEE, 2014, pp. 4059–4064.

[7] E. Vanet, S. Touré, N. Kechagia, R. Caire, and N. HadjSaid, "Sensitivity analysis of local flexibilities for voltage regulation in unbalanced lv distribution system," in *2015 IEEE Eindhoven PowerTech*. IEEE, 2015, pp. 1–6.

[8] B. B. Zad, J. Lobry, and F. Vallée, "A new voltage sensitivity analysis method for medium-voltage distribution systems incorporating power losses impact," *Electric Power Components and Systems*, vol. 46, no. 14-15, pp. 1540–1553, 2018.

[9] E. Demirok, P. C. Gonzalez, K. H. Frederiksen, D. Sera, P. Rodriguez, and R. Teodorescu, "Local reactive power control methods for overvoltage prevention of distributed solar inverters in low-voltage grids," *IEEE Journal of Photovoltaics*, vol. 1, no. 2, pp. 174–182, 2011.

[10] Z. Zhang, L. F. Ochoa, and G. Valverde, "A novel voltage sensitivity approach for the decentralized control of dg plants," *IEEE Transactions on Power Systems*, vol. 33, no. 2, pp. 1566–1576, 2017.

[11] Q. Tao, D. Wang, B. Yang, H. Liu, and S. Yan, "Voltage control of distribution network with distributed generation based on voltage sensitivity matrix," in *2018 IEEE International Conference on Energy Internet (ICEI)*. IEEE, 2018, pp. 298–302.

[12] S. Hashemi, J. Østergaard, and G. Yang, "A scenario-based approach for energy storage capacity determination in lv grids with high pv penetration," *IEEE Transactions on Smart Grid*, vol. 5, no. 3, pp. 1514–1522, 2014.

[13] A. Giannitrapani, S. Paoletti, A. Vicino, and D. Zarrilli, "Optimal allocation of energy storage systems for voltage control in lv distribution networks," *IEEE Transactions on Smart Grid*, vol. 8, no. 6, pp. 2859–2870, 2016.

[14] S. Shafiq, B. Khan, and A. T. Al-Awami, "Optimal battery placement in distribution network using voltage sensitivity approach," in *2019 IEEE Power and Energy Conference at Illinois (PECI)*. IEEE, 2019, pp. 1–4.

[15] M. R. Montanés, J. R. Santos, and E. R. Ramos, "Voltage sensitivity based technique for optimal placement of switched capacitors," in *15th PSCC*, 2005, pp. 22–26.

[16] G. De Carne, M. Liserre, and C. Vournas, "On-line load sensitivity identification in lv distribution grids," *IEEE Transactions on Power Systems*, vol. 32, no. 2, pp. 1570–1571, 2016.

[17] D. Croop. Performance scoring. [Online]. Available: https://tinyurl.com/79xf8xhr

[18] S. S. Torbaghan, G. Suryanarayana, H. Höschle, R. D'hulst, F. Geth, C. Caerts, and D. Van Hertem, "Optimal flexibility dispatch problem using second-order cone relaxation of ac power flows," *IEEE Transactions on Power Systems*, vol. 35, no. 1, pp. 98–108, 2019.

[19] K. Christakou, J.-Y. LeBoudec, M. Paolone, and D.-C. Tomozei, "Efficient computation of sensitivity coefficients of node voltages and line currents in unbalanced radial electrical distribution networks," *IEEE Transactions on Smart Grid*, vol. 4, no. 2, pp. 741–750, 2013.

[20] S. Weckx, C. Gonzalez, and J. Driesen, "Combined central and local active and reactive power control of pv inverters," *IEEE Transactions on Sustainable Energy*, vol. 5, no. 3, pp. 776–784, 2014.

[21] S. Karagiannopoulos, P. Aristidou, and G. Hug, "Hybrid approach for planning and operating active distribution grids," *IET Generation, Transmission & Distribution*, vol. 11, no. 3, pp. 685–695, 2017.

[22] A. R. Malekpour and A. Pahwa, "A dynamic operational scheme for residential pv smart inverters," *IEEE Transactions on Smart Grid*, vol. 8, no. 5, pp. 2258–2267, 2016.

[23] R. A. Jabr, "Radial distribution load flow using conic programming," *IEEE trans. on power systems*, vol. 21, no. 3, pp. 1458–1459, 2006.

[24] C. Coffrin, R. Bent, K. Sundar, Y. Ng, and M. Lubin, "Powermodels. jl: An open-source framework for exploring power flow formulations," in *2018 Power Systems Computation Conference (PSCC)*. IEEE, 2018, pp. 1–8.